



Since January 2020 Elsevier has created a COVID-19 resource centre with free information in English and Mandarin on the novel coronavirus COVID-19. The COVID-19 resource centre is hosted on Elsevier Connect, the company's public news and information website.

Elsevier hereby grants permission to make all its COVID-19-related research that is available on the COVID-19 resource centre - including this research content - immediately available in PubMed Central and other publicly funded repositories, such as the WHO COVID database with rights for unrestricted research re-use and analyses in any form or by any means with acknowledgement of the original source. These permissions are granted for free by Elsevier for as long as the COVID-19 resource centre remains active.



ELSEVIER

Contents lists available at ScienceDirect

Heart & Lung

journal homepage: www.heartandlung.com

Predictive value of initial CT scan for various adverse outcomes in patients with COVID-19 pneumonia

Bardia Khosravi, MD^a, Leila Aghaghazvini, MD^b, Majid Sorouri, MD^a, Sara Naybandi Atashi, MD^b, Mohammad Abdollahi, MD^a, Helia Mojtavavi, MD^a, Marjan Khodabakhshi, MD^a, Fatemeh Motamedi, MD^a, Fatemeh Azizi, MD^a, Zeynab Rajabi, MD^a, Amir Kasaeian, PhD^c, Ali Reza Sima, MD^a, Amir H. Davarpanah, MD^d, Amir Reza Radmard, MD^{b,*}

^a Digestive Diseases Research Center, Digestive Diseases Research Institute, Tehran University of Medical Sciences, Tehran, Iran

^b Department of Radiology, Shariati Hospital, Tehran University of Medical Sciences, North Kargar St., Tehran 14117, Iran

^c Hematology, Oncology and Stem Cell Transplantation Research Center, Tehran University of Medical Sciences, Tehran, Iran

^d Department of Radiology and Imaging Sciences, Emory University School of Medicine, Atlanta, USA

ARTICLE INFO

Article History:

Received 9 June 2020

Revised 1 October 2020

Accepted 6 October 2020

Available online 14 October 2020

Keywords:

COVID-19

CT scan

Intubation

ICU Admission

Mortality

ABSTRACT

Background: Chest computed tomography (CT) scan is frequently used in the diagnosis of COVID-19 pneumonia.

Objectives: This study investigates the predictive value of CT severity score (CSS) for length-of-stay (LOS) in hospital, initial disease severity, ICU admission, intubation, and mortality.

Methods: In this retrospective study, initial CT scans of consecutively admitted patients with COVID-19 pneumonia were reviewed in a tertiary hospital. The association of CSS with the severity of disease upon admission and the final adverse outcomes was assessed using Pearson's correlation test and logistic regression, respectively.

Results: Total of 121 patients (60±16 years), including 54 women and 67 men, with positive RT-PCR tests were enrolled. We found a significant but weak correlation between CSS and qSOFA, as a measure of disease severity ($r: 0.261, p = 0.003$). No significant association was demonstrated between CSS and LOS. Patients with CSS>8 had at least three-fold higher risk of ICU admission, intubation, and mortality.

Conclusions: CSS in baseline CT scan of patients with COVID-19 pneumonia can predict adverse outcomes and is weakly correlated with initial disease severity.

© 2020 Elsevier Inc. All rights reserved.

Introduction

In late 2019, clustered pneumonia cases were reported from the city of Wuhan in the Hubei province of China. Later in January 2020, WHO declared this issue as a public health emergency of international concern (PHEIC),¹ and the disease itself was named COVID-19. Later the virus was designated as SARS-CoV-2 relating to its predecessor SARS-CoV, responsible for the SARS epidemic in 2003. On February 18, 2020, Iran's first case of COVID-19 was reported from Qom city. Later, in March 2020, WHO declared COVID-19 a pandemic. Until

June 1, 2020, more than 160,000 confirmed cases were reported from Iran and globally confirmed cases rose to 6.4 million.²

The primary receptor of SARS-CoV-2 entrance is the ACE-2 protein, which is abundant in alveolar tissue, making the lungs the primary target of the disease.³ COVID-19 usually presents with fever and respiratory symptoms such as cough, sputum, and dyspnea.^{4,5} A Lung CT scan has been shown to have a 94% sensitivity in relation to the RT-PCR test.⁶ This makes baseline CT scan a powerful diagnostic tool for rapid triage of suspected patients with COVID-19 in resource-constrained settings⁷ like Iran, where RT-PCR kits are not widely available, or their results are reported much later than the time of admission.

Since January 2020, multiple studies have been published describing the CT findings of COVID-19 patients suggesting a correlation of CT findings with disease severity or outcome.^{8–10} So far, a few scoring systems had been used to quantify lung involvement of COVID-19 patients.^{11–14} However, the prognostic value of radiologic findings

Abbreviations: SARS-CoV-2, severe acute respiratory syndrome coronavirus 2; COVID-19, coronavirus disease 19; RT-PCR, reverse-transcription polymerase chain reaction; CSS, CT severity score; qSOFA, quick sequential organ failure assessment; LOS, length of stay

* Corresponding author.

E-mail address: radmard@tums.ac.ir (A.R. Radmard).

<https://doi.org/10.1016/j.hrtlng.2020.10.005>

0147-9563/© 2020 Elsevier Inc. All rights reserved.

on outcomes has not been investigated thoroughly. In the current study, we describe initial CT findings of inpatient COVID-19 pneumonia cases and assess its predictive value for clinical outcomes, including length of stay (LOS), ICU admission, intubation, and mortality. We also investigate the prognostic value of baseline CT severity score (CSS) to predict the disease's severity and the mentioned outcome measures.

Material and method

Patient population and study design

This is a retrospective study conducted in a tertiary referral hospital, Tehran, Iran. The study has been approved by the ethical committee of Tehran University of Medical Sciences (IRB approval number: IR.TUMS.VCR.REC.1399.002), and participation consent was not required as the study used retrospective data. We reviewed all chest CT studies performed in the hospital inpatient imaging center between February 18, 2020, and April 19, 2020. All scans had been initially triaged upon admission by the on-call radiologist, with experience of at least five years. Patients with scans suggestive of COVID-19 had been considered for possible admission. According to the national COVID-19 protocol, all suspected patients (having suggestive scans) with respiratory symptoms and at least one of the following criteria were admitted to the hospital: (a) O₂ saturation < 93% (b) tachypnea (respiratory rate \geq 22) (c) tachycardia (pulse rate > 100) (d) hypotension (systolic blood pressure \leq 100 mmHg).

All scans of admitted patients were reviewed again, from April 20 to April 25, by three experienced radiologists in consensus, actively involved in reporting suspected COVID-19 pneumonia cases over the past two months. All patients whose initial scans were not highly suggestive of COVID-19, based on national diagnostic criteria,¹⁵ were excluded.

We then reviewed the patients' medical records. Those patients who met the following inclusion criteria were enrolled in this study: (a) presenting symptoms favoring COVID-19 diagnosis in congruence with WHO interim guideline (b) positive SARS-CoV-2 RT-PCR results, (c) available laboratory data. We excluded patients who have not been discharged until April 19, 2020. The flowchart of the patient enrollment process is depicted in Fig. 1.

Clinical data

We extracted the patients' initial vital signs, including temperature, respiratory rate, blood pressure, O₂ saturation, and initial laboratory data from hospital medical records. While the supervising physician double-checked the clinical data upon entry, the extraction of laboratory data was conducted using an automated computer program to minimize any error during the process. The qSOFA score, used for the rapid evaluation of patients suspected with sepsis.¹⁶ Further detail regarding laboratory data definitions is provided in Table 1. The time gap between initial clinical assessment, laboratory test sampling, and scans was negligible (< 12 h) for all enrolled patients.

Four outcome measures were defined for patients: (a) whether they were alive and discharged or have deceased, (b) whether at any point of admission needed ICU care, (c) whether have been intubated during admission, (d) the LOS.

CT acquisition technique

All chest scans were non-enhanced and were performed during inspiratory breath-hold at the supine position, using a 16-detector-row CT scanner (Philips Brilliance 16, Philips Medical Systems, Best, the Netherlands). Our CT acquisition protocol was as follows: tube

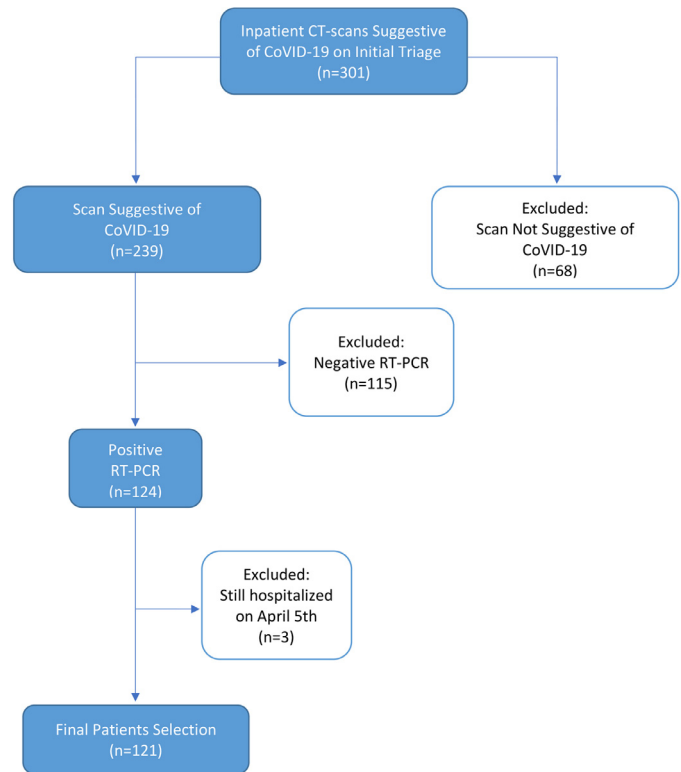


Fig. 1. Flowchart of the patient enrollment process. Abbreviations: RT-PCR, reverse-transcription polymerase chain reaction.

Table 1
Demographic, clinical, and laboratory data definitions.

Variable	Definition
Older Adults	Age > 64 years
Fever	Oral temperature greater than 37.5 °C
Hypoxia	O ₂ saturation < 93%
qSOFA	1 score if GCS < 15 1 score if SBP \leq 100 mmHg 1 score if RR \geq 22
Lymphopenia	Absolute lymphocyte count of less than 1000/mm ³
Neutrophilia	Absolute neutrophil count of more than 7700/mm ³
Thrombocytopenia	Plt count less than 150,000/mm ³
Anemia	HB level of less than 12 gr/dL in women HB level of less than 14 gr/dL in men
CRP	Values less than 5 mg/L
AST	Values greater than 40 U/L
Coagulopathy	INR > 1.1

Abbreviations: SBP, systolic blood pressure; RR: respiratory rate; eGFR, estimated glomerular filtration rate; CRP, C-reactive protein; AST, aspartate transaminase; INR, international normalized ratio of prothrombin time; HB, hemoglobin; Plt, platelet.

voltage, 100 kV if patients' BMI \leq 30 and 120 kV for patients with BMI > 30; tube current, 45 mAs; pitch, 1; collimation, 16 \times 1.5 mm; increment, 1.5; Matrix, 512. Images were reconstructed with 3 mm slice thickness using both sharp kernels (filter "L") with a lung window (1500 width; -350 center) and medium-soft kernels (filter "B") with a soft-tissue window (400 width; 60 center).

CT image analysis

After initial triage of all chest CT scans by the on-call radiologist upon admission, based on the diagnostic criteria of Iranian society of radiology,¹⁵ scans with findings highly suggestive of COVID-19 were retrospectively evaluated by two radiologists in consensus, with 5 and 12 years of experience (S.N. and L.A. respectively), blind to

patient outcomes. A third radiologist with 12 years of experience (A. R.), settled any controversy. The following characteristics were reported: (a) type of parenchymal abnormality, including (i) ground-glass opacities (GGO) (ii) consolidation, (iii) reticular pattern, (iv) honeycomb formation; (b) type of GGO; (c) axial and craniocaudal distribution; (d) pleural effusion; (e) pericardial effusion; (f) emphysema; (g) bronchiectasis; (h) fibrosis; (i) pneumothorax; (j) cardiomegaly; (k) mediastinal lymphadenopathy (short-axis diameter > 10 mm). All individuals with either bronchiectasis, emphysema, or fibrosis were considered to have underlying lung disease. Patients with coronary artery stent or atherosclerotic plaque in scans were presumed to have coronary heart disease.

Additionally, each lung was divided into three zones, (a) upper zone (above the level of carina), (b) middle zone (between the carina and inferior pulmonary vein), and (c) lower zone (below the level of the inferior pulmonary vein). Each zone was evaluated for the percentage of involvement by either of the mentioned parenchymal abnormalities and was assigned a score from 0 to 4, 0: no involvement, 1: 1–25% involved, 2: 26–50% involved, 3: 51–75% involved, 4: 76–100% involved. The final CT severity score (CSS) was calculated by summing the scores from all six zones yielding a score between 0 and 24.

Statistical analysis

All statistical analysis was performed with *Stata Statistical Software*, release 14, StataCorp LLC. We used logistic regression univariable and multivariable analysis. After univariable analysis, all variables in congruence with prior evidence and a p-value < 0.1 were entered into the multivariable model. The receiving operator characteristic (ROC) curve was drawn to demonstrate the multivariable models' predictive capability. We used Pearson's correlation test to measure the association between CSS, qSOFA, and LOS. A p-value < 0.05 was considered significant in all instances. We compared the mean of LOS in high and low CSS sub-groups using an independent sample T-test. We present continuous variables as median (IQR) and categorical variables as number (percent).

Results

Descriptive analysis

Table 2 summarizes demographic, clinical, and laboratory findings in different outcome sub-groups. After the exclusion of 3 patients (due to hospitalization; Fig. 1), the study included 121 patients (54 women, 44.6%; 67 men, 55.4%) with a mean age of 60.29 (SD: 15.93). Among our patients, 47 were ICU admitted (38.8%), 38 were intubated (31.4%), and 36 have deceased (29.7%). ICU admitted patients had a median age of 64 (IQR: 54–70), while intubated, and deceased patients had a median age of 67 (IQR: 56–73 and 57–72.5, respectively). Upon admission, 8/121 patients (6.6%) had a qSOFA score \geq 2, 7 of which eventually were intubated and deceased. In laboratory findings, 56/121 (46.3%) patients had anemia, and 47/121 (38.8%) patients had lymphopenia. Anemia prevalence was 28/47 (59.6%), 26/38 (68.4%), and 24/36 (66.7%) in ICU admitted, intubated, and deceased patients, respectively. Lymphopenia was observed in 25/47 (53.2%) ICU admitted patients, 19/38 (50.0%) intubated patients, and 18/36 (50.0%) deceased patients. The median LOS was 6 days (IQR: 3–11).

Radiologic findings are summarized in Table 3. The most prevalent abnormality patterns observed were GGO and consolidation, 110/121 (90.9%), and 96/121 (79.3%), respectively. As only one patient had honeycombing formation, this parameter was excluded in further analysis. Most scans revealed interlobular septal thickening on the background of GGO, 62/121 (56.4%). Of 121 patients, 67 (55.4%) had no craniocaudal dominance in parenchymal abnormality distribution. Only 8/121 (6.6%) patients showed unilateral lung involvement. Right lower, 114/121 (94.2%), and left lower, 111/121 (91.7%) were involved most frequently. Underlying lung disease was observed in 20/121 (20.7%) patients who had emphysema, fibrosis, or bronchiectasis. Cardiomegaly was reported in 67/121 (55.4%) patients. Coronary heart disease, either a coronary stent or atherosclerotic plaque, was evident in 11/121 (9.1%) patients. The median CSS was 8 (IQR: 5–14). We used this median as the threshold for further analysis of CSS in all instances. CSS median in ICU admitted, intubated, and deceased patients were 11 (IQR: 6–18), 12 (IQR: 6–18),

Table 2
Demographic, clinical and laboratory findings.

Variable	All (n = 121)	ICU Admitted (n = 47)	Intubated (n = 38)	Deceased (n = 36)
Sex				
Women	54 (44.6%)	19 (40.4%)	14 (36.8%)	12 (33.3%)
Men	67 (55.4%)	28 (59.6%)	24 (63.2%)	24 (66.7%)
Age (years)	61 (52–70)	64 (54–70)	67 (56–73)	67 (57–72.5)
\geq 65	52 (43.0%)	23 (48.9%)	22 (57.9%)	21 (58.3%)
O ₂ Saturation (%)	92 (88–95)	89 (79–95)	88.5 (75–95)	87.5 (73–95)
< 93	70 (57.8%)	30 (63.8%)	25 (65.8%)	25 (66.7%)
Temperature (°C)	37 (36.8–38.4)	37 (36.8–38.8)	37 (36.8–38.5)	37 (36.8–38.65)
> 37.5	49 (40.5%)	19 (40.4%)	16 (42.1%)	15 (41.7%)
CRP (mg/L)	61 (25–82)	78.0 (40–85.4)	79.9 (40–83)	79.9 (40–89.5)
> 5	114 (94.2%)	44 (93.6%)	36 (94.7%)	34 (94.4%)
AST (units/L)	39 (31–51)	47 (34–70.5)	48 (34–67)	48 (34–74)
> 40	67 (55.4%)	29 (61.7%)	25 (65.8%)	24 (66.7%)
INR	1.26 (1.11–1.43)	1.29 (1.14–1.41)	1.29 (1.14–1.42)	1.29 (1.14–1.43)
Coagulopathy	97 (80.2%)	39 (83.0%)	32 (84.2%)	31 (86.1%)
HB (gr/dL)	12.6 (10.9–14.7)	12.0 (10.1–14.1)	11.2 (10.0–13.2)	11.3 (9.6–13.6)
Anemia	56 (46.3%)	28 (59.6%)	26 (68.4%)	24 (66.7%)
Plt (*10 ³ /mm ³)	176 (110–231)	152 (101–225)	155 (105–189)	155 (105.5–195)
Thrombocytopenia	49 (40.5%)	23 (48.9%)	18 (47.4%)	17 (47.2%)
Lymph (/mm ³)	1026 (651–1500)	910 (525–1206)	953 (504–1206)	953 (504–1206)
Lymphopenia	47 (38.8%)	25 (53.2%)	19 (50.0%)	18 (50.0%)
Neutr (/mm ³)	4383 (2870–7560)	5091 (3182–9296)	5510 (3654–11,385)	5382 (3654–9296)
Neutrophilia	44 (36.4%)	18 (38.3%)	15 (39.5%)	14 (38.9%)

Continuous variables are presented as median (IQR) and categorical variables are presented as number (percent). Abbreviations: CRP, C-reactive protein; AST, aspartate transaminase; INR, international normalized ratio of prothrombin time; HB, hemoglobin; Plt, platelet; Lymph, lymphocyte count in peripheral blood; Neutr, neutrophil count in peripheral blood.

Table 3
Radiologic findings.

Variable	All(n = 121)	ICU Admitted(n = 47)	Intubated(n = 38)	Deceased(n = 36)
Abnormality Type				
GGO	110 (90.9%)	41 (87.2%)	33 (86.8%)	31 (86.1%)
Consolidation	96 (79.3%)	41 (87.2%)	33 (86.8%)	32 (88.9%)
Reticular Pattern	34 (28.1%)	8 (17.0%)	7 (18.4%)	6 (16.7%)
HC Pattern	1 (0.8%)	0 (0%)	0 (0%)	0 (0%)
GGO Type				
Pure GGO	18 (16.4%)	7 (17.0%)	6 (18.8%)	6 (19.4%)
IST + GGO	62 (56.4%)	23 (56.1%)	17 (51.5%)	15 (48.4%)
AD + GGO	11 (10.0%)	6 (14.6%)	5 (15.1%)	5 (16.1%)
CP	19 (17.3%)	5 (12.2%)	5 (15.1%)	5 (16.1%)
Axial Distribution				
Subpleural	66 (54.5%)	27 (57.4%)	23 (60.5%)	21 (58.3%)
Central	4 (3.3%)	1 (2.1%)	1 (2.6%)	1 (2.8%)
Diffuse	51 (42.15%)	19 (40.4%)	14 (36.8%)	14 (38.9%)
Craniocaudal Distribution				
Apical	5 (4.1%)	3 (6.4%)	3 (7.9%)	3 (8.3%)
Basal	49 (40.5%)	20 (42.6%)	14 (36.8%)	12 (33.3%)
No Dominance	67 (55.4%)	24 (51.0%)	21 (55.3%)	21 (58.4%)
Bilateral Involvement	113 (93.4%)	46 (97.9%)	37 (97.4%)	35 (97.2%)
Involved Zones				
Right Upper	92 (76.0%)	38 (80.8%)	30 (79.0%)	29 (80.6%)
Right Middle	99 (81.8%)	39 (83.0%)	32 (84.2%)	31 (86.1%)
Right Lower	114 (94.2%)	46 (97.9%)	37 (97.4%)	35 (97.2%)
Left Upper	82 (67.8%)	36 (76.6%)	29 (76.3%)	29 (80.6%)
Left Middle	98 (81.0%)	41 (87.2%)	34 (89.5%)	33 (91.7%)
Left Lower	111 (91.7%)	46 (97.9%)	37 (97.4%)	35 (97.2%)
Pleural Effusion	26 (21.7%)	14 (29.8%)	12 (31.6%)	12 (33.3%)
Pericardial Effusion	18 (14.9%)	8 (17.0%)	7 (18.4%)	7 (19.4%)
Underlying Lung Disease	25 (20.7%)	7 (14.9%)	5 (13.2%)	5 (13.9%)
Pneumothorax	1 (0.8%)	1 (2.1%)	1 (2.7%)	1 (2.9%)
Cardiomegaly	67 (55.4%)	27 (57.4%)	22 (57.9%)	22 (61.1%)
Mediastinal Lymphadenopathy	6 (5.0%)	3 (6.4%)	2 (5.3%)	2 (5.6%)
Coronary Heart Disease	11 (9.1%)	2 (4.3%)	1 (2.6%)	1 (2.8%)
Number of Zones Involved	6 (4–6)	6 (5–6)	6 (5–6)	6 (5–6)
CSS	8 (5–14)	11 (6–18)	12 (6–18)	12 (7.5–19)

Continuous variables are presented as median (IQR) and categorical variables are presented as number(percent). Abbreviations: GGO, ground-glass opacity; HC: honeycomb formation, IST, interlobular septal thickening; CP, crazy paving pattern; AD, architectural distortion; CSS, CT severity score.

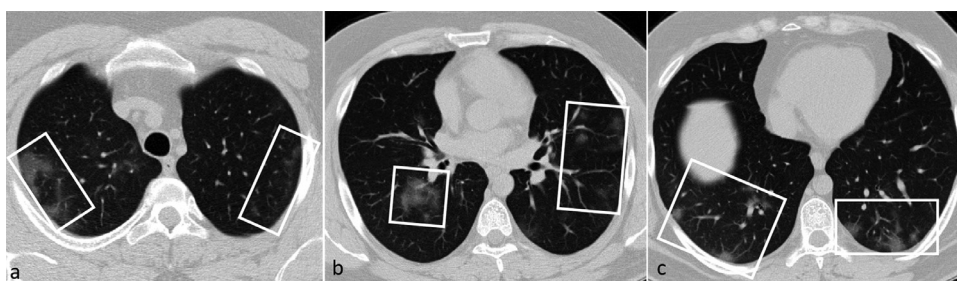


Fig. 2. A 34-year-old man presented with a dry cough, myalgia, and fever for two days. There are multifocal patchy and nodular ground-glass opacities, mostly peripherally located (boxes). The total CSS was calculated as 6. He was discharged on day 6 of admission without the need for ICU care or intubation.

and 12 (IQR: 7.5–19), respectively. We found a significant but weak correlation between CSS and qSOFA ($r: 0.261$, p -value: 0.003). CSS and LOS were not significantly correlated (p -value: 0.829) in our patients. Meanwhile, the mean LOS was not significantly different between patients with high and low CSS (p -values: 0.970). **Fig. 2** shows some sections of a patient's scan with mild lung involvement. **Figs. 3** and **4** depict patients' scans with moderate and severe lung involvements, respectively.

Logistic regression analysis

Table 4 summarizes the results of the univariable analysis in different outcome sub-groups. Older patients were significantly more

frequent in intubation (p -value: 0.027) and mortality (p -value: 0.028) groups. Anemia was significantly more common in patients with unfavorable outcomes.

Of radiologic findings, $CSS > 8$ (OR: 3.00, 95% CI: 1.40–6.44, p -value: 0.005) and presence of reticular pattern in initial scans (OR: 0.37, 95% CI: 0.15–0.92, p -value: 0.034) could predict ICU admission, the latter having protective effect. A $CSS > 8$ was also associated with higher mortality (OR: 3.9, 95% CI: 1.66–9.11, p -value: 0.002) and intubation (OR: 3.12, 95% CI: 1.38–7.03, p -value: 0.006) in our patients.

All variables with a p -value < 0.1 in univariable analysis were entered into a multivariable model to independently predict outcome measures and measure their association. The final results are

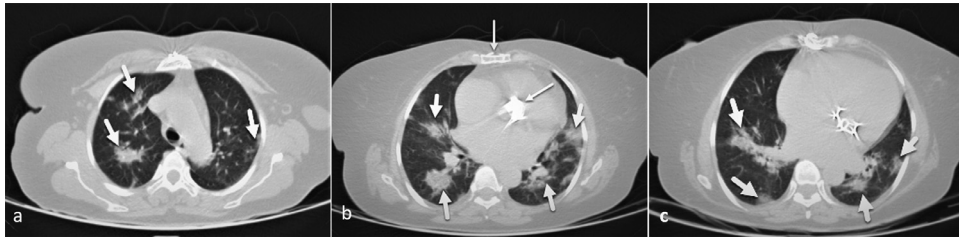


Fig. 3. A 59-year-old woman presented with dyspnea and fever and O₂ saturation of 85%. There are multifocal bilateral patchy ground-glass opacities and consolidations (thick arrows), with the central and peripheral distribution. Findings of the previous sternotomy and mitral and aortic valve replacement are depicted along with mild cardiomegaly (thin arrows). The total CSS was calculated as 9. The patient was admitted to the ICU and intubated; however, she eventually discharged on day 15 of admission.



Fig. 4. A 64-year-old man presented with severe dyspnea, fever, and O₂ saturation of 81%. There are diffuse bilateral confluent ground-glass opacities and consolidations in both lungs (thick arrows) resembling the ARDS pattern. Cardiomegaly is also evident (thin arrow). The total CSS was calculated as 22, and the patient passed away on day 8 of admission following ICU admission and intubation.

presented in Table 5, and Fig. 5. Anemia was associated with higher mortality (p -value: 0.004), intubation (p -value: 0.001) and ICU admission (p -value: 0.015). Moreover, presence of reticular pattern was negatively associated with ICU admission and mortality with an OR of 0.37 (95% CI: 0.13–0.99, p -value: 0.049) and an OR of 0.32 (95% CI: 0.10–0.99, p -value: 0.049) respectively. CSS > 8 was positively associated with all three outcomes in our patients and could predict them. The best predictive value was demonstrated to predict mortality (OR: 5.29, 95% CI: 1.44–19.32, p -value: 0.012).

Discussion

Hospitalized patients with COVID-19 may eventually need ICU admission (27%), intubation (19%), or even face mortality (17%) during their admission.¹⁷ The ability to predict these outcomes based on initial scans gives physicians a better insight to manage patients with COVID-19. In this study, we used a CT severity score, CSS, for patients' baseline scans to predict the outcomes mentioned above. Having a CSS > 8 in RT-PCR positive COVID-19 patients predicts ICU admission with an OR of 3.68 (95% CI: 1.18–11.48), intubation with an OR of 3.36 (95% CI: 1.35–8.35) and mortality with an OR of 5.29 (95% CI: 1.44–19.32). Presence of reticular pattern in lung CT scans, has a protective effect against ICU admission (OR: 0.37, 95% CI: 0.13–0.99) and mortality (OR: 0.32, 95% CI: 0.10–0.99). Although the proposed scoring system may have some flaws with our sample size, we used this model to lay a ground for further research regarding the predictive value of the proposed system.

Multiple demographic and clinical factors have been proposed to predict unfavorable outcome in patients with COVID-19. In a study by Huang et al., patients with unfavorable outcome were significantly older, had a higher qSOFA score, and were lymphopenic.¹⁸ We found similar results in our study. We also found a weak correlation between CSS and qSOFA score, suggesting that this radiologic score is not a reliable measure to show initial disease severity, but can predict the outcome. No association was found between CSS and LOS outcomes. This can be attributed to other reasons for a prolonged stay, such as superimposed complications (e.g., nosocomial infections, thromboembolic events, or electrolyte disturbance), which might not

be associated with the percentage of lung involvement in baseline CT scans.

In concordance with previous reports, most of our patients had bilateral lung involvement, with GGO and consolidation being the most frequent abnormality. Lower zones were also the most frequently involved anatomical location in this study.^{10,19,20} Our findings suggest that patients with a reticular pattern in their baseline CT scans will have smaller odds of being intubated or facing mortality. This can be attributed to the evidence that reticular abnormalities appear later in the course of the disease; hence, patients with an initial reticular pattern may have passed the critical period of the infection.^{21,22}

We used a modified version of the scoring system proposed by Zhou et al. to make it more feasible and rapidly achievable in clinical practice.²² Patients with CSS > 8 in baseline scans had at least three folds higher risk of poor outcomes, including ICU admission, intubation, and mortality. Other scoring systems have also been proposed to predict the prognosis of patients with COVID-19. Pan et al. proposed a scoring system based on the number of lobes and percentages of involvement in each lobe.²³ Although widely adopted by other studies,^{24,25} we believe that this system was not suitable as the final score was not linearly associated with total lung involvement. Colombi et al. used a software-based calculation of aerated lung volume to predict ICU admission or death.²⁶ Ufuk et al. used the area of pectoralis major muscles in CT scans to predict the severity of the COVID pneumonia outcomes.²⁷ Although the latter two mentioned studies have had promising results, they are more applicable in a research setting rather than a clinical one. Yuan et al. have proposed a scoring system based on the type of abnormality and the area involved by each type with reliable results in predicting mortality. However their sample size was limited to a total of 27 patients and a mortality rate of 37%.²⁸ Our scoring system can be easily implemented for clinical use, and our sample size would suffice to deduce its validity.

This study was conducted with an appropriate sample volume and laboratory and clinical data. To the best of our knowledge, the association of these three outcomes with initial CT findings has not been well established in the literature. In addition to mortality, CSS

Table 4
Univariable analysis of clinical, laboratory and radiologic findings.

Variable	ICU Admission (n = 47)		Intubation (n = 38)		Mortality (n = 36)	
	OR(95% CI)	p-value	OR(95% CI)	p-value	OR(95% CI)	p-value
Clinical and Lab Findings						
Age ≥ 65	1.48 (0.71–3.11)	0.292	2.42 (1.10–5.32)	0.027 ^{†*}	2.43 (1.09–5.40)	0.028 ^{†*}
O ₂ Saturation < 93%	1.50 (0.70–3.17)	0.290	1.62 (0.73–3.60)	0.233	1.69 (0.75–3.82)	0.203
Temperature > 37.5 °C	0.99 (0.47–2.09)	0.990	1.10 (0.50–2.40)	0.807	1.07 (0.48–2.36)	0.864
CRP > 5 mg/L	0.83 (0.17–3.92)	0.823	1.15 (0.21–6.23)	0.868	1.06 (0.19–5.74)	0.944
AST > 40 units/L	1.52 (0.72–3.21)	0.265	1.87 (0.84–4.16)	0.121	1.95 (0.86–4.40)	0.106
Coagulopathy	1.34 (0.52–3.44)	0.537	1.47 (0.53–4.08)	0.452	1.78 (0.61–5.22)	0.290
Anemia	2.42 (1.14–5.11)	0.021 ^{†*}	3.82 (1.68–8.66)	0.001 ^{†*}	3.31 (1.45–7.52)	0.004 ^{†*}
Thrombocytopenia	1.76 (0.84–3.72)	0.133	1.50 (0.69–3.28)	0.299	1.48 (0.67–3.25)	0.328
Lymphopenia	2.68 (1.25–5.74)	0.011 ^{†*}	1.96 (0.89–4.29)	0.091 [†]	1.93 (0.87–4.26)	0.104
Neutrophilia	1.14 (0.53–2.44)	0.725	1.21 (0.55–2.68)	0.631	1.66 (0.53–2.60)	0.707
Radiologic Findings						
GGO	0.49 (0.14–1.72)	0.270	0.51 (0.14–1.80)	0.299	0.47 (0.13–1.65)	0.240
Consolidation	2.36 (0.86–6.43)	0.093 [†]	0.209 (0.72–6.08)	0.174	2.62 (0.83–8.29)	0.100
Reticular Pattern	0.37 (0.15–0.92)	0.034 ^{†*}	0.46 (0.18–1.19)	0.114	0.40 (0.15–1.09)	0.074 [†]
GGO Type						
Pure GGO	Ref.	Ref.	Ref.	Ref.	Ref.	Ref.
IST + GGO	0.92 (0.31–2.72)	0.890	0.75 (0.24–2.33)	0.626	0.63 (0.99–1.99)	0.440
AD + GGO	1.88 (0.41–8.61)	0.413	1.66 (0.35–7.76)	0.515	1.66 (0.35–7.76)	0.515
CP	0.56 (0.13–2.26)	0.416	0.71 (0.17–2.94)	0.641	0.71 (0.17–2.94)	0.641
Axial Distribution						
Subpleural	Ref.	Ref.	Ref.	Ref.	Ref.	Ref.
Central	0.48 (0.04–4.87)	0.536	0.62 (0.06–6.33)	0.689	0.71 (0.07–7.28)	0.776
Diffuse	0.85 (0.40–1.81)	0.688	0.70 (0.31–1.56)	0.394	0.81 (0.36–1.81)	0.609
Craniocaudal Distribution						
Apical	Ref.	Ref.	Ref.	Ref.	Ref.	Ref.
Basal	0.45 (0.07–3.00)	0.417	0.17 (0.40–1.77)	0.171	0.21 (0.03–1.45)	0.115
No Dominance	0.37 (0.25–8.97)	0.297	0.30 (0.04–1.95)	0.211	0.30 (0.04–1.95)	0.211
Bilateral Involvement	4.80 (0.57–40.3)	0.148	3.40 (0.40–28.7)	0.260	3.14 (0.37–26.50)	0.293
Pleural Effusion	2.15 (0.89–5.19)	0.087 [†]	2.24 (0.91–5.47)	0.077 [†]	2.5 (1.01–6.14)	0.046 ^{†*}
Pericardial Effusion	1.34 (0.48–3.70)	0.58	1.52 (0.54–4.31)	0.424	1.68 (0.59–4.77)	0.98
Underlying Lung Disease	0.54 (0.20–1.42)	0.216	0.47 (0.16–1.38)	0.174	0.52 (0.17–1.52)	0.236
Cardiomegaly	1.14 (0.54–2.39)	0.714	1.16 (0.53–2.52)	0.706	1.39 (0.63–3.09)	0.409
Mediastinal Lymphadenopathy	1.59 (0.30–8.23)	0.580	1.08 (0.18–6.18)	0.928	1.17 (0.20–6.73)	0.855
Coronary Heart Disease	0.32 (0.06–1.55)	0.158	0.19 (0.02–1.60)	0.129	0.21 (0.02–1.74)	0.149
Number of Zones Involved	1.27 (0.97–1.66)	0.078 [†]	1.24 (0.93–1.66)	0.130	1.34 (0.98–1.84)	0.059 [†]
CSS (continuous)	1.15 (1.07–1.23)	<0.001 [*]	1.14 (1.06–1.22)	<0.001 [*]	1.17 (1.08–1.26)	<0.001 [*]
CSS > 5 [‡]	1.99 (0.87–4.53)	0.101	1.82 (0.76–4.36)	0.177	2.00 (0.81–4.94)	0.129
CSS > 8 [§]	3.00 (1.40–6.44)	0.005 ^{†*}	3.12 (1.38–7.03)	0.006 ^{†*}	3.9 (1.66–9.11)	0.002 ^{†*}
CSS > 12 [‡]	3.18 (1.38–7.34)	0.007 [*]	3.66 (1.56–8.58)	0.003 [*]	4.17 (1.76–9.86)	0.001 [*]

[†] 25th Percentile of CSS was 5.

[§] Median of CSS was 8.

[‡] 75th Percentile of CSS was 12.

[†] Entered into multivariable analysis.

^{*} Significant p-value

Abbreviations: CRP, C-reactive protein; AST, aspartate transaminase; INR, international normalized ratio of prothrombin time; HB, hemoglobin; Plt, platelet; Lymph, lymphocyte count in peripheral blood; Neutr, neutrophil count in peripheral blood; GGO, ground-glass opacity; HC: honeycomb formation, IST, interlobular septal thickening; CP, crazy paving pattern; AD, architectural distortion; CSS, CT severity score.

Table 5
Final results of multivariable analysis.

Outcome	Variable	OR(95% CI)	p-value	AUC
ICU Admission (n = 47)	Lymphopenia	2.37 (1.01–5.54)	0.045*	0.762
	Anemia	2.92 (1.23–6.92)	0.015*	
	Reticular Pattern in Scan	0.37 (0.13–0.99)	0.049*	
	CSS > 8	3.68 (1.18–11.48)	0.025*	
Intubation (n = 38)	Age ≥ 65	2.86 (1.17–6.98)	0.021*	0.791
	Anemia	4.62 (1.84–11.58)	0.001*	
	CSS > 8	3.36 (1.35–8.35)	0.009*	
Mortality (n = 36)	Age ≥ 65	2.81 (1.12–7.03)	0.026*	0.792
	Anemia	3.86 (1.52–9.77)	0.004*	
	Reticular Pattern in Scan	0.32 (0.10–0.99)	0.049*	
	CSS > 8	5.29 (1.44–19.32)	0.012*	

* Significant p-value

Abbreviations: CC, craniocaudal; CSS, CT severity score.

could predict intubation and ICU admission, outcomes which may have higher cost and burden for the healthcare system. Putting resource constraints together with the considerable delay in providing RT-PCR results, CSS can be useful for patients' management and predict outcomes. Although extensive study is required, CSS might be helpful to decide how early certain treatments such as corticosteroids

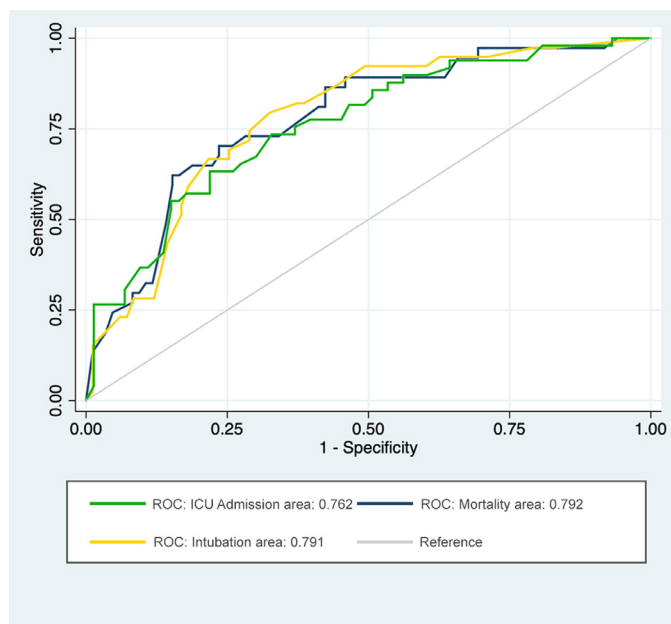


Fig. 5. ROC curves based on predictive models for outcomes including: lymphopenia, anemia, reticular pattern, and CSS > 8 to predict ICU admission; age, anemia, and CSS > 8 to predict intubation; age, anemia, reticular pattern, and CSS > 8 to predict mortality.

or anti-viral agents should start for patients with COVID-19 pneumonia. Also, this score might be able to predict late post-infection complications such as lung fibrosis or other kinds of interstitial lung diseases (ILDs).

However, our findings are subject to some limitations. First, it was a retrospective study that needs to be investigated with further

multicenter prospective studies. Second, due to RT-PCR kit shortages in the initial days of the COVID-19 epidemic in Iran, RT-PCR testing was not performed for 18 patients, and they were excluded from the study. Third, nasopharyngeal sampling errors due to the anxiety and overly protective measures in the first few weeks had increased the rate of false-negative RT-PCR results. Finally, due to the extra workload caused by the pandemic, we did not perform a third re-evaluation of the CT scan data in order to calculate the intra-observer reliability.

In conclusion, baseline CT findings can predict final patient outcomes, including ICU admission, intubation, and mortality. Having reticular abnormalities predicts a better outcome. Although CT severity score, CSS, of baseline CT scans is weakly correlated with disease severity upon admission, it can predict ICU admission, intubation, and mortality in COVID-19 patients in an inpatient setting. Clinicians and radiologists can use CSS as a measure of disease severity and an indicator of poor outcome, including the need of mechanical ventilation. Also, observing reticular pattern upon admission can be interpreted as a reassuring radiologic sign. We suggest further research regarding the reliability and predictive value of CSS using multicenter prospective studies. We also encourage the investigation of the effect of different treatment regimens in patients in different CSS groups.

Declarations of Competing Interest

None.

Acknowledgment

This project is not supported by national or private funding, and all authors contribute solely as volunteers. We dedicate our results to all radiographers, nurses, and physicians all around the world and especially in Iran, who are risking their lives to manage this tough situation.

References

- WHO Main Website [Internet]. 2020. Available from: <https://www.who.int>.
- WHO. Coronavirus disease 2019 (COVID-19), Report-111 [Internet]. 2020. Available from: https://www.who.int/docs/default-source/coronaviruse/situation-reports/20200510covid-19-sitrep-111.pdf?sfvrsn=1896976f_2.
- Zhao Y, Zhao Z, Wang Y, Zhou Y, Ma Y, Zuo W. Single-Cell RNA Expression Profiling of ACE2, the Receptor of SARS-CoV-2. *bioRxiv* [Internet]. 2020;2020.01.26.919985. Available from: <http://biorxiv.org/content/early/2020/04/09/2020.01.26.919985.abstract>.
- Li L-Q, Huang T, Wang Y-Q, et al. 2019 novel coronavirus patients' clinical characteristics, discharge rate and fatality rate of meta-analysis. *J Med Virol*. 2020;92:577–583. Available from: <http://www.ncbi.nlm.nih.gov/pubmed/32162702>.
- Weiss P, Murdoch DR. Clinical course and mortality risk of severe COVID-19. *Lancet*. 2020;2019(20):2019–2020. Available from: <http://www.ncbi.nlm.nih.gov/pubmed/32197108>.
- Kim H, Hong H, Yoon SH. Diagnostic performance of CT and reverse transcriptase-polymerase chain reaction for coronavirus disease 2019: a meta-analysis. *Radiology*. 2020;80:(2) 201343. Available from: <https://doi.org/10.1148/radiol.2020201343>.
- Rubin GD, Haramati LB, Kanne JP, et al. The role of chest imaging in patient management during the COVID-19 pandemic: a multinational consensus statement from the Fleischner society. *Radiology*. 2020;296:172–180.
- Pan F, Ye T, Sun P, Gui S, Liang B, Li L, et al. Time course of lung changes on chest CT during recovery from 2019 novel coronavirus (COVID-19) pneumonia. *Radiology*. 2020 200370. Available from: <https://doi.org/10.1148/radiol.2020200370>.
- Yoon SH, Lee KH, Kim JY, et al. Chest radiographic and CT findings of the 2019 novel coronavirus disease (COVID-19): analysis of nine patients treated in Korea. *Korean J Radiol*. 2020;21(822):1–7. Available from: <https://www.kjronline.org/DOIx.php?id=10.3348/kjr.2020.0132>.
- Kanne JP. Chest CT findings in 2019 novel coronavirus (2019-nCoV) infections from Wuhan, China: key points for the radiologist. *Radiology*. 2020 200241. Available from: <https://doi.org/10.1148/radiol.202020241>.
- Wu J, Wu X, Zeng W, et al. Chest CT findings in patients with corona virus disease 2019 and its relationship with clinical features. *Investig Radiol*. 2020;55:257–261. Available from: <http://www.ncbi.nlm.nih.gov/pubmed/32091414>.

12. Feng F, Jiang Y, Yuan M, Shen J, Yin H, Geng D, et al. Association of radiologic findings with mortality in patients with avian influenza H7N9 pneumonia. *PLoS One*. 2014;9(4):1–8.
13. Li K, Fang Y, Li W, et al. CT image visual quantitative evaluation and clinical classification of coronavirus disease (COVID-19). *Eur Radiol*. 2020;30:4407–4416. Available from: <http://www.ncbi.nlm.nih.gov/pubmed/32215691>.
14. Yang R, Li X, Liu H, et al. Chest CT severity score: an imaging tool for assessing severe COVID-19. *Radiol Cardiothorac Imaging*. 2020;2:(2) e200047. Available from: <https://doi.org/10.1148/radiol.2016152244>.
15. Mahdavi A, Khalili N, Davarpanah AH, et al. Radiologic management of COVID-19: preliminary experience of the Iranian society of radiology COVID-19 consultant group (ISRCC). *Iran J Radiol*. 2020;17(2):17–19.
16. Seymour CW, Liu VX, Iwashyna TJ, et al. Assessment of clinical criteria for sepsis. *JAMA*. 2016;315(8):762. Available from: <https://doi.org/10.1001/jama.2016.0288>.
17. Yang X, Yu Y, Xu J, et al. Clinical course and outcomes of critically ill patients with SARS-CoV-2 pneumonia in Wuhan, China: a single-centered, retrospective, observational study. *Lancet Respir Med*. 2020;2600(20):1–7. Available from: [https://doi.org/10.1016/S2213-2600\(20\)30079-5](https://doi.org/10.1016/S2213-2600(20)30079-5).
18. Huang C, Wang Y, Li X, et al. Clinical features of patients infected with 2019 novel coronavirus in Wuhan, China. *Lancet*. 2020;395(10223):497–506.
19. Li M, Lei P, Zeng B, et al. Coronavirus disease (COVID-19): spectrum of CT findings and temporal progression of the disease. *Acad Radiol*. 2020;(10):1–6. Available from: <https://doi.org/10.1016/j.acra.2020.03.003>.
20. Xiong Y, Sun D, Liu Y, et al. Clinical and High-Resolution CT Features of the COVID-19 Infection: Comparison of the Initial and Follow-up Changes. *Invest Radiol*. 2020;55(6):332–339.
21. Shi H, Han X, Jiang N, et al. Radiological findings from 81 patients with COVID-19 pneumonia in Wuhan, China: a descriptive study. *Lancet Infect Dis*. 2020;3099(20):1–10. Available from: [https://doi.org/10.1016/S1473-3099\(20\)30086-4](https://doi.org/10.1016/S1473-3099(20)30086-4).
22. Zhou S, Wang Y, Zhu T, Xia L. CT features of coronavirus disease 2019 (COVID-19) pneumonia in 62 Patients in Wuhan, China. *AJR Am J Roentgenol*. 2020;214:1287–1294.
23. Pan F, Ye T, Sun P, et al. Time course of lung changes at chest CT during recovery from coronavirus disease 2019 (COVID-19). *Radiology*. 2020;295(3):715–721. Available from: <https://doi.org/10.1148/radiol.2020200370>.
24. Francone M, lafrate F, Masci GM, et al. Chest CT score in COVID-19 patients: correlation with disease severity and short-term prognosis. *Eur Radiol*. 2020. Available from: <http://www.ncbi.nlm.nih.gov/pubmed/32623505>.
25. Raoufi M, Safavi Naini SAA, Azizan Z, et al. Correlation between chest computed tomography scan findings and mortality of COVID-19 cases; a cross sectional study. *Arch Acad Emerg Med*. 2020;8(1):e57. Available from: <http://www.ncbi.nlm.nih.gov/pubmed/32613199%0Ahttp://www.pubmedcentral.nih.gov/articlerender.fcgi?artid=PMC7305634>.
26. Colombi D, Bodini FC, Petrini M, et al. Well-aerated lung on admitting chest CT to predict adverse outcome in COVID-19 pneumonia. *Radiology*. 2020;80:(2) 201433. Available from: <https://doi.org/10.1148/radiol.2020201433>.
27. Ufuk F, Demirci M, Sagtas E, Akbudak IH, Ugurlu E, Sari T. The prognostic value of pneumonia severity score and pectoralis muscle Area on chest CT in adult COVID-19 patients. *Eur J Radiol*. 2020;131: 109271. Available from: <http://www.science-direct.com/science/article/pii/S0720048X20304605>.
28. Yuan M, Yin W, Tao Z, Tan W, Hu Y. Association of Radiologic Findings with Mortality of Patients Infected with 2019 Novel Coronavirus in Wuhan, China. medRxiv 2020;2020.02.22.20024927. Available from: <http://dx.doi.org/10.1371/journal.pone.0230548>.